



Title	Zero temperature coefficient of sound velocity in vitreous silicon oxynitride thin films
Author(s)	Nagakubo, A.; Tsuboi, S.; Kabe, Y. et al.
Citation	Applied Physics Letters. 2019, 114(25), p. 251905-1-251905-5
Version Type	VoR
URL	https://hdl.handle.net/11094/83932
rights	Copyright 2019 Author(s). This article may be downloaded for personal use only. Any other use requires prior permission of the author and AIP Publishing. This article appeared in Applied Physics Letters, 114(25), 251905, 2019 and may be found at https://doi.org/10.1063/1.5098354 .
Note	

The University of Osaka Institutional Knowledge Archive : OUKA

<https://ir.library.osaka-u.ac.jp/>

The University of Osaka

Zero temperature coefficient of sound velocity in vitreous silicon oxynitride thin films

Cite as: Appl. Phys. Lett. **114**, 251905 (2019); <https://doi.org/10.1063/1.5098354>

Submitted: 02 April 2019 . Accepted: 05 June 2019 . Published Online: 25 June 2019

A. Nagakubo, S. Tsuboi, Y. Kabe, S. Matsuda, A. Koreeda, Y. Fujii , and H. Ogi



View Online



Export Citation



CrossMark

Lock-in Amplifiers up to 600 MHz

starting at

\$6,210



 Zurich Instruments

Watch the Video



AIP
Publishing

Zero temperature coefficient of sound velocity in vitreous silicon oxynitride thin films

Cite as: Appl. Phys. Lett. **114**, 251905 (2019); doi: [10.1063/1.5098354](https://doi.org/10.1063/1.5098354)

Submitted: 2 April 2019 · Accepted: 5 June 2019 ·

Published Online: 25 June 2019



View Online



Export Citation



CrossMark

A. Nagakubo,¹ S. Tsuboi,² Y. Kabe,³ S. Matsuda,³ A. Koreeda,⁴ Y. Fujii,⁴  and H. Ogi^{1,a)}

AFFILIATIONS

¹Graduate School of Engineering, Osaka University, 2-1 Yamadaoka, Suita, Osaka 565-0871, Japan

²Graduate School of Engineering Science, Osaka University, Toyonaka, Osaka 560-8531, Japan

³Skyworks Solutions, Inc., Kadoma, Osaka 571-0050, Japan

⁴Department of Physical Sciences, Ritsumeikan University, Shiga 525-8577, Japan

^{a)}E-mail: ogi@prec.eng.osaka-u.ac.jp

ABSTRACT

Vitreous silicon oxide ($v\text{-SiO}_2$) shows anomalous phonon properties such as the positive temperature coefficient of velocity (TCV). Variation of the Si–O–Si bond angle between SiO_4 tetrahedrons has been recognized to be the key, but the origin of TCV still remains unclear. In this study, we controlled the bond angle by doping nitrogen and measured TCV of vitreous silicon oxynitride thin films with various nitrogen concentrations using picosecond ultrasonics. TCV significantly decreases by adding a small amount of nitrogen, and it shows positive to negative values as the nitrogen concentration increases. We evaluated the bond-angle change by Fourier-transform infrared spectroscopy, which decreases with the increase in the nitrogen content. We also find that the temperature rise in nondoped $v\text{-SiO}_2$ decreases the bond angle, leading to an increase in the sound velocity. We then reveal theoretically that the bond-angle change dominates the origin of the positive TCV. This study indicates the existence of a zero-TCV single material, and we discover that the specific content of $v\text{-SiO}_{1.71}\text{N}_{0.19}$ achieves this.

Published under license by AIP Publishing. <https://doi.org/10.1063/1.5098354>

Usually, heating a material causes volume expansion due to the anharmonicity of lattices, and the mass density decreases, resulting in softening of the material. The elastic constants thus decrease as temperature increases, and because this contribution is more significant than the mass-density decrease, the sound velocity also decreases. This behavior appears commonly in most materials, including metals and semiconductors. On the other hand, vitreous silicon dioxide ($v\text{-SiO}_2$) exhibits a positive temperature coefficient of velocity (TCV)¹ near room temperature despite positive thermal expansion.² This unusual characteristic is applied to many applications to compensate the sound-velocity change with temperature variation. For example, $v\text{-SiO}_2$ thin film is often deposited on acoustic-wave filters to improve their temperature stability.

The positive TCV of $v\text{-SiO}_2$ has been well known since the 1950s.^{1,3,4} This material exhibits negative TCV below 100 K, but it is caused by structural relaxation and anharmonic damping effects, and it was estimated that $v\text{-SiO}_2$ would exhibit positive TCV even at low temperatures without these effects.^{4,5} Thus, the positive TCV is an essential characteristic of $v\text{-SiO}_2$. Krause and Kurkjian⁶ found that vitreous materials [SiO_2 , GeO_2 , BeF_2 , and $\text{Zn}(\text{PO}_3)_2$], showing the

tetrahedral structure, commonly exhibit positive thermal expansion coefficient and positive TCV, while B_2O_3 , showing the planar triangle structure, exhibits negative TCV, indicating the importance of the tetrahedral structure in achieving the positive TCV. In the 1970s, the gigahertz-range measurement with the Brillouin scattering method⁷ was performed, which confirmed the identical positive TCV value near room temperature even at very high frequencies. Kulbitskaya and co-authors postulated that structural inhomogeneities in glass softened the material and its effect would decrease with the temperature increase, leading to positive TCV.^{8,9} However, this model could not explain the TCV behavior of some tetrahedron-structure glasses.⁵ Even in the 1990s, many authors mentioned that the origin of positive TCV has not been understood,^{10,11} although they recognize that the lateral vibration of O^{12,13} and the SiO_4 tetrahedron structure¹¹ are important factors. In glassy materials, two or more amorphous states could coexist and their proportions are dependent on temperature,¹⁴ and Huang and Kieffer performed molecular dynamics simulations and concluded that the unusual sound velocity change can be caused by spontaneous Si–O–Si bond rotations in the α – β amorphous phase transition.^{15,16} Moreover, they mentioned that the reduction of

Si–O–Si angle θ could not be the direct reason for the positive TCV, although their calculation predicted a decrease in the bond angle with the temperature increase.

It is therefore unambiguously important that the bond angle between the tetrahedron units will dominate the unusual properties of v-SiO₂. However, there is no systematic study on the correlation between TCV and the bond angle. In this study, to reveal the origin of the positive TCV, we measure sound velocity of vitreous silicon oxynitride (v-SiO_xN_y) films between 10 and 300 K by picosecond ultrasonics and evaluate the bond-angle change by Raman spectroscopy and Fourier-transform infrared (FT-IR) spectroscopy. Since nitrogen atoms can have three bonds to Si atoms, while oxygen atoms have two bonds, the Si–N–Si bond angle becomes smaller than the Si–O–Si angle θ , so that we can control θ by doping N into v-SiO₂. Because vitreous silicon nitride, v-Si₃N₄, exhibits negative (usual) TCV,¹⁷ by increasing the N atoms, we will observe a positive-to-negative change of TCV, which provides us with important information on the positive TCV mechanism. Furthermore, this approach will reveal a zero-TCV single material. (Note that achieving the zero-TCV required a composite consisting of a positive TCV material such as v-SiO₂ and negative TCV materials.)

We synthesized v-SiO_xN_y films on (100) Si substrates by a reactive sputtering method with a Si target under an Ar/N₂/O₂ atmosphere.¹⁸ We controlled the composition by changing the flow rates of Ar, N₂, and O₂ gases; it was determined by the X-ray photoelectron spectroscopy (XPS) method as follows: The binding energy of the Si(2p) bond changes with the content ratios of N and O between 101 and 103 eV,¹⁹ and we determined the content ratios of O and N to Si from the spectrum-area ratios of O(1s) and N(1s) to Si(2p), respectively (Fig. S1 in the [supplementary material](#)). Here, we define N_r as the nitrogen ratio $N_r = N/(O + N)$. The mass density ρ of the thin film was determined by the X-ray reflectivity method²⁰ (Fig. S2). The measured ρ values are shown in Table I and Fig. 1(a). Despite smaller atomic mass of N than that of O, ρ increases as the nitrogen ratio N_r

TABLE I. Determined mass density ρ , sound velocity v , longitudinal elastic constant C_L , TCV, and ω_4 of each film with reference values. N_r denotes the nitrogen ratio [$N_r = N/(O + N)$].

Specimen	N_r	ρ (kg/m ³)	v (km/s)	C_L (GPa)	TCV (ppm/K)	ω_4 (cm ⁻¹)
SiN _{4/3}	1	3020 ^a	10.206 ^b	314.5 ^{a,b}	-21.0 ^{a,b}	
SiO _{0.13} N _{0.09}	0.891	2940	10.083	298.3	-15.3	886.1
SiO _{0.36} N _{0.96}	0.726	2910	9.877	282.6	-14.4	898.2
SiO _{0.67} N _{0.83}	0.552	2810	9.401	248.3	-24.1	960.5
SiO _{0.94} N _{0.63}	0.402	2680	8.823	208.6	-14.2	974.4
SiO _{1.24} N _{0.44}	0.260	2690	8.342	187.2	-8.14	996.7
SiO _{1.71} N _{0.19}	0.101	2510	7.496	141.0	-0.64	1030.9
SiO _{1.77} N _{0.11}	0.059	2390	7.124	121.3	11.8	1041.4
SiO _{1.93} N _{0.07}	0.035	2370	6.837	110.8	56.5	1048.1
SiO ₂	0	2220 ^c	5.967 ^d	79.0 ^{c,d}	69.9 ^d	1064.5 ^d

^aReference 17.

^bReference 27.

^cReference 25.

^dReference 26.

increases, indicating that the averaged bond angle becomes smaller. We confirmed that these films do not show any crystalline phases with X-ray diffraction (XRD) spectra as shown in the [supplementary material](#) (Fig. S3), where only the Si (100) peaks for Co-K α and Co-K β X-ray appear except for noise signals.

We measured the longitudinal-wave sound velocity v by picosecond ultrasonics,^{21,22} which is the pump-probe laser ultrasonics with a femtosecond pulse laser. We used a titanium/sapphire pulse laser whose wavelength and repetition rate were about 800 nm and 80 MHz, respectively. The light pulse was divided into pump and probe light pulses by a polarization beam splitter. The pump light path was controlled by corner reflectors and a stage controller, and we modulated the pump light at 100 kHz for the lock-in-amplifier detection. The wavelength of the probe light was converted into 400 nm by a second harmonic generator. Both light normally entered a specimen in a cryostat through an objective lens and a glass window.²³

We deposited Al thin films on the specimens as the transducer, which absorbed pump light pulses and excited strain pulses. The strain pulse diffracts the probe light backward, whose wave vector satisfies Bragg's condition. The diffracted light interferes with reflected light from the surface, and therefore, total intensity is modulated with strain-pulse propagation as the frequency of $f = 2nv/\lambda$, where λ is the wavelength of the probe light and n is the refractive index of the specimen.²⁴ This oscillation is called Brillouin oscillation. We measured n of the v-SiO_xN_y films and λ by ellipsometry and a spectrometer, respectively.

We show waveforms observed at room temperature in Fig. 2(a). The strain pulse generated at the surface propagates in a v-SiO_xN_y film, causing the Brillouin oscillation, and reaches the Si substrate around 100–180 ps. The transmitted strain pulse causes the Brillouin oscillation in Si. The reflected strain pulse propagates in the v-SiO_xN_y film backward, reflects at the surface, and reaches the Si substrate again as shown in Figs. 2(b)–2(d). At room temperature, we determined the sound velocity from the Brillouin-oscillation frequency by applying

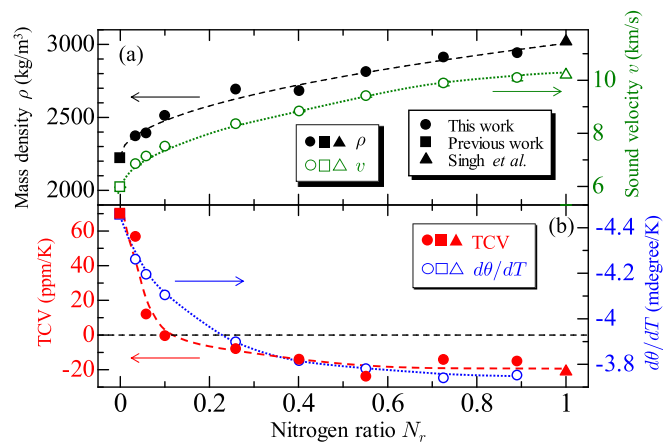


FIG. 1. (a) Dependence of mass density ρ (black solid symbols) and sound velocity v (green open symbols). (b) Dependence of the temperature coefficient of velocity TCV (red solid symbols) and temperature coefficient of the bond angle $d\theta/dT$ (blue open symbols). Circles are the measured values in this work, and squares and triangles are the reported values for v-SiO₂^{25,26} and v-SiN_{4/3},^{17,27} respectively. The lines are guides to the eye. The arrow indicates the axis to be referred.

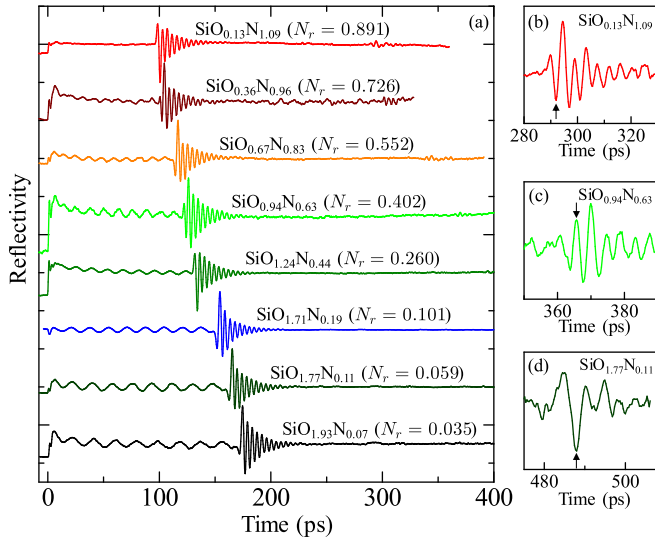


FIG. 2. (a) Observed acoustic signals in v-SiO_xN_y thin films at room temperature. Brillouin oscillation of v-SiO_xN_y first appears, and the following large-amplitude and high-frequency signals are those of the Si substrate. We evaluated the round trip time by using the second Brillouin oscillation at the Si substrate denoted by the arrows in (b)–(d).

fast Fourier transform and obtained the longitudinal-wave elastic constant $C_L = \rho v^2$, which is shown in Table I. The sound velocity is depicted in Fig. 1(a), together with reference values.^{17,25–27} As the nitrogen ratio increases, the mass density increases because of reduction of the bond angles between polyhedrons (angles of O–Si–O, O–Si–N, and N–Si–N), leading to the decrease in the averaged atomic distance. This causes the significant increase in the elastic modulus. We here focus on the O–Si–O bond angle, because it is a representative characteristic related to changes in those bond angles, and it is accurately obtainable by the FT-IR and Raman spectroscopy.

In measuring TCV, we determined the sound velocity change Δv by the pulse-echo method not by the Brillouin oscillation,²⁸ because the temperature coefficient of n (~ 8 ppm/K)²⁹ is larger than thermal expansion coefficient α_t (~ 0.4 ppm/K)² and it is difficult to accurately measure the temperature dependence of n . On the other hand, the thickness change is suppressed because of the cancelation between thermal expansion and Poisson's effect of the film, and its influence on the velocity measurement is negligible;²⁸ the thermal expansion coefficient α_t of a thin film deposited on a substrate is modified as $\alpha_t - 2C_{12}(\alpha_t^{\text{Sub}} - \alpha_t)/C_{11}$ by assuming the biaxial stress condition, where C_{12} and C_{11} are the isotropic elastic constants of the film and α_t^{Sub} is the thermal expansion coefficient of the substrate. This evaluation, for example, estimates the film-thickness change of 0.03% or less for a v-SiO₂ film on Si caused by a 100-K temperature variation, which is only one twentieth of the velocity change. Therefore, we propose to measure the velocity in v-SiO_xN_y films thanks to a time-of-flight measurement.

The arrow in Figs. 2(b)–2(d) indicates the second arrival time to the Si substrate. (We chose a clearly visible peak of the signal to determine the arrival time. A small difference in the sampling point has a negligible influence in determining TCV because it is derived from the relative velocity change.) We then measured the one-and-half round

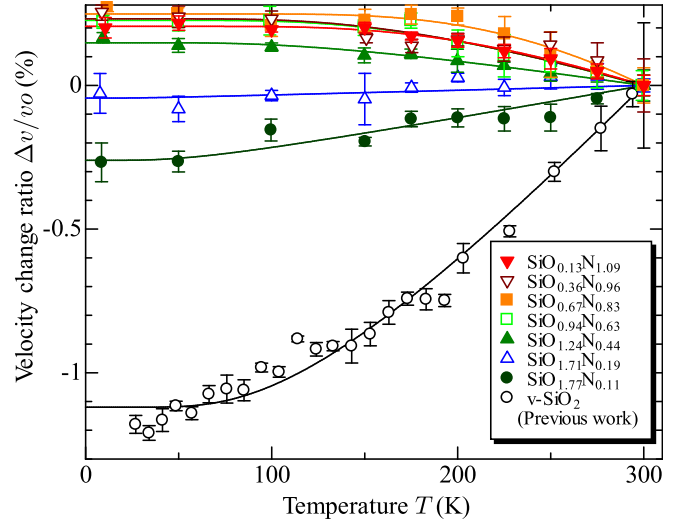


FIG. 3. Sound velocity change ratios $\Delta v/v_0$ of v-SiO_xN_y films from the room-temperature values determined by the pulse-echo method. Values of pure v-SiO₂ were obtained from our previous work.²⁶

trip time and determined Δv from room temperature as shown in Fig. 3. A pure v-SiO₂ film shows positive TCV,²⁶ but TCV of the v-SiO_xN_y film decreases as the nitrogen ratio N_r increases. We determined TCV using data between 200 and 300 K, which are shown in Table I and Fig. 1(b). As the nitrogen content increases, the TCV value changes from positive to negative as expected. However, the zero-TCV film is achieved at a very low N_r value ($N_r \sim 0.1$), which is unexpected behavior because the absolute value of TCV of v-SiO₂ is three-times higher than that of v-SiN [Fig. 1(b)], and a large amount of nitrogen was expected to achieve the zero TCV. TCV is, thus, highly affected by the addition of nitrogen atoms near $N_r = 0$, and we attribute this unusual TCV behavior to the bond-angle temperature coefficient as shown below.

To reveal the origin of the positive TCV of v-SiO₂, we measured the Raman spectrum of a bulk v-SiO₂ between 77 and 373 K (Fig. S4). Tetrahedral glasses have four representative phonon modes (ω_1 , ω_2 , ω_3 , and ω_4), which significantly depend on the bond angle θ .³⁰ Among them, we used the ω_3 and ω_4 modes to evaluate the bond-angle change: the ω_1 mode is close to a defect line D_1 which arises from the symmetric stretch and irregular planar glass network, and the ω_2 peak overlaps on the broad ω_1 peak^{31,32} (Fig. S4). The frequencies of ω_3 and ω_4 modes are given by

$$\omega_3 = \sqrt{\frac{C(1 + \cos \theta)}{m_O} + \frac{4C}{3m_{Si}}}, \quad (1)$$

$$\omega_4 = \sqrt{\frac{C(1 - \cos \theta)}{m_O} + \frac{4C}{3m_{Si}}}, \quad (2)$$

where m_O and m_{Si} are the mass of O and Si atoms, respectively, and C is the spring constant for the Si–O bond stretching.³⁰ Both ω_3 and ω_4 peaks exhibit transverse-optical (TO) and longitudinal-optical (LO) modes.^{31,32} We determined their phonon frequencies for the ω_3 mode using the double-peak function-fitting method. On the other hand, the TO and LO modes of the ω_4 peak are clearly separated, and we

measured the phonon frequency of the TO- ω_4 mode. With the temperature increase, phonon frequencies of the ω_3 and ω_4 modes increase and decrease, respectively, as shown in Fig. 4(a). We inversely calculated the bond angle θ and the spring constant C from the measured phonon frequencies of the TO- ω_3 mode (lower ω_3 mode) and TO- ω_4 mode as shown in Fig. 4(b), which agree with those reported with $\sim 5\%$ or less.³³ We find that they decrease as temperature increases. The spring constant, thus, decreases as temperature increases as like usual materials, and, therefore, the decrease in θ should cause the sound-velocity increase with the temperature increase.

In our previous study, we made several v-SiO₂ films with different sputtering powers and found that v increases as θ decreases.²⁵ Importantly, the bond-angle change caused by temperature and sputtering power leads to an identical sound-velocity change: In the previous measurement, $dv/d\omega_4$ is estimated to be -0.29 m/s.²⁵ On the other hand, the reported TCV (dv/dT)²⁶ and the temperature dependence of the ω_4 frequency $d\omega_4/dT$ yield the $dv/d\omega_4$ value of -0.25 m/s. They well agree with each other, indicating that the sound velocity change is principally governed by the change in the Si-O-Si bond angle.

We consider that this structural change governs TCV of the v-SiO_xN_y film. To evaluate the bond-angle change, we measured the FT-IR spectra of the films. We observed superimposed spectra of Si-N and Si-O absorption peaks around 1000 cm^{-1} and determined the peak frequency of the ω_4 mode by the multipeak function-fitting method [Figs. S5(a) and S5(b)]. With an increase in the nitrogen ratio N_r , the peak frequency linearly decreases [Fig. S5(c)], which corresponds to a gradual decrease in the bond angle θ . We reveal that the unexpected nitrogen-ratio dependence of TCV is explained by the temperature coefficient of the bond angle $d\theta/dT$: by differentiating ω_4^2 [Eq. (2)] with respect to T , $d\theta/dT$ becomes

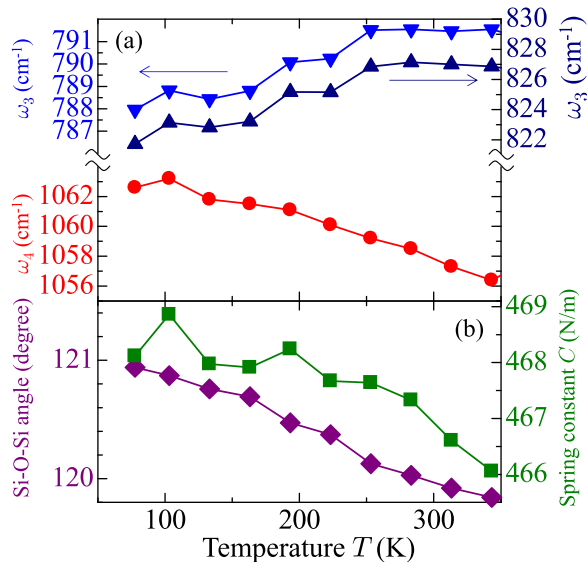


FIG. 4. (a) Temperature dependence of the Raman shift for the ω_3 (blue triangles) and TO- ω_4 modes (red circles) in v-SiO₂. (b) We determined the temperature dependence of the Si-O-Si bond angle (purple diamond) and the spring constant C of the Si-O bond (green square) from the measured ω_3 and ω_4 . The arrow indicates the axis to be referred.

$$\frac{d\theta}{dT} = \frac{m_O}{C \sin \theta} \left\{ 2\omega_4 \frac{d\omega_4}{dT} - \left(\frac{1 - \cos \theta}{m_O} + \frac{4}{3m_{\text{Si}}} \right) \frac{dC}{dT} \right\}, \quad (3)$$

and we calculated $d\theta/dT$ values of v-SiO_xN_y films using dC/dT and $d\omega_4/dT$ values of pure v-SiO₂ in Fig. 4. (These temperature coefficients were determined using experiments between 190 and 340 K.) We show the calculated $d\theta/dT$ values in Fig. 1(b). TCV and $d\theta/dT$ show a similar dependence on the nitrogen ratio N_r , and they show a good correlation (inset in Fig. 5).

The bond angle in the v-SiO_xN_y film is expected to decrease with the temperature increase as seen in v-SiO₂, which contributes to an increase in v . However, when the bond angle is already small enough due to the existence of N atoms, the absolute value of its temperature coefficient $|d\theta/dT|$ becomes small, whereas the interatomic bond length becomes larger because of thermal expansion, which contributes to the decrease in v . Therefore, the TCV value is determined by the trade-off between the two conflicting mechanisms: the bond-angle change and thermal expansion. The zero-TCV v-SiO_xN_y film can then be realized by the exact balance between the two factors. The most important point is that TCV of vitreous SiO₂-base materials does not seem to depend on the doped atoms but only on the bond angle temperature coefficient: we show the ω_4 -frequency dependence of TCV of v-SiO_xN_y and v-SiO_{2-z}F_z²⁶ films in Fig. 5. With an increase in the phonon frequency, TCV of the film increases. This behavior can be explained by the temperature coefficient of the bond angle as shown in the inset, where the $d\theta/dT$ value shows a linear correlation with TCV even involving the F-doped films.

To conclude, we synthesized v-SiO_xN_y films and measured their sound velocity between 10 and 300 K using time-of-flight measurements using the picosecond ultrasonic technique. Doping N atoms caused an increase in sound velocity and a decrease in TCV. We evaluated the structural change from the TO- ω_4 phonon frequency, which corresponds to the Si-O-Si bond angle. We conclude that the change of the bond angle is the most important parameter for governing TCV of v-SiO_xN_y and v-SiO_{2-z}F_z ($z < 0.264$). The temperature increase

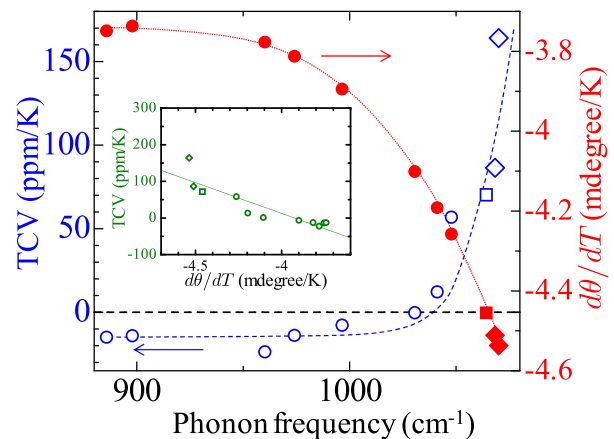


FIG. 5. Phonon-frequency dependence of TCV (blue open symbols) and $d\theta/dT$ (red solid symbols) of v-SiO_xN_y (circle), v-SiO_{2.26} (square), and v-SiO_{2.26}F_{z.26} films (diamond). The lines are guides to the eye. The inset shows the relationship between $d\theta/dT$ and TCV, where the solid line is the least squares line. The arrow indicates the axis to be referred.

leads to a decrease in the bond angle, resulting in positive TCV. However, if it already becomes small enough, it cannot become smaller even with temperature increase, and usual thermal expansion causes a decrease in mass density and sound velocity. Thus, the TCV of $v\text{-SiO}_x\text{N}_y$ is determined by the trade-off between the two conflicting factors: the change in the bond angle and thermal expansion. The zero TCV single material can then be realized by adjusting the doping quantity, and we reveal it to be $v\text{-SiO}_{1.71}\text{N}_{0.19}$.

See the [supplementary material](#) for XPS, x-ray-reflectivity, XRD, Raman, and FT-IR measurements.

REFERENCES

- ¹H. J. McSkimin, *J. Appl. Phys.* **24**, 988 (1953).
- ²G. K. White, *J. Phys. D* **6**, 2070 (1973).
- ³J. W. Marx and J. M. Sivertsen, *J. Appl. Phys.* **24**, 81 (1953); M. E. Fine, H. V. Duyne, and N. T. Kenney, *ibid.* **25**, 402 (1954); S. Spinner, *J. Am. Ceram. Soc.* **39**, 113 (1956); A. Polian, D. V. Thanh, and P. Richet, *Europhys. Lett.* **57**, 375 (2002).
- ⁴O. L. Anderson and H. E. Bömmel, *J. Am. Ceram. Soc.* **38**, 125 (1955).
- ⁵R. Vacher, E. Courtens, and M. Foret, *Phys. Rev. B* **72**, 214205 (2005); B. Rufflé, S. Ayirinhac, E. Courtens, R. Vacher, M. Foret, A. Wischnewski, and U. Buchenau, *Phys. Rev. Lett.* **104**, 067402 (2010); S. Ayirinhac, B. Rufflé, M. Foret, H. Tran, S. Clément, R. Vialla, R. Vacher, J. C. Chervin, P. Munsch, and A. Polian, *Phys. Rev. B* **84**, 024201 (2011).
- ⁶J. T. Krause and C. R. Kurkjian, *J. Am. Ceram. Soc.* **51**, 226 (1968).
- ⁷A. S. Pine, *Phys. Rev.* **185**, 1187 (1969); W. Heinicke, G. Winterling, and K. Dransfeld, *J. Acoust. Soc. Am.* **49**, 954 (1971); J. T. Krause, *Phys. Lett.* **43**, 325 (1973); J. Pelous and R. Vacher, *Solid State Commun.* **16**, 279 (1975); R. Vacher and J. Pelous, *Phys. Rev. B* **14**, 823 (1976).
- ⁸M. N. Kulbitskaya, S. V. Nemilov, and V. A. Shutilov, *Sov. Phys. Solid State* **16**, 2319 (1975).
- ⁹M. N. Kulbitskaya and V. A. Shutilov, *Sov. Phys. Acoust.* **22**, 451 (1976).
- ¹⁰R. Vacher, J. Pelous, F. Plicque, and A. Zarembowitch, *J. Non-Cryst. Solids* **45**, 397 (1981); K. Doring, S. Rau, G. Weiss, J. Arndt, and S. Hunklinger, *Phys. Lett. A* **184**, 464 (1994).
- ¹¹S. Hunklinger, *J. Phys.* **43**, C9-461 (1982).
- ¹²H. J. Stevens, *J. Non-Cryst. Solids* **38**, 487 (1980).
- ¹³K. Hirao, K. Tanaka, S. Furukawa, and N. Soda, *J. Sci. Mater. Lett.* **14**, 697 (1995).
- ¹⁴M. R. Vukcevic, *J. Non-Cryst. Solids* **11**, 25 (1972).
- ¹⁵L. Huang and J. Kieffer, *Phys. Rev. B* **69**, 224203 (2004).
- ¹⁶L. Huang and J. Kieffer, *Phys. Rev. B* **69**, 224204 (2004).
- ¹⁷K. J. Singh, Y. Matsuda, K. Hattori, H. Nakano, and S. Nagai, *Ultrasonics* **41**, 9 (2003).
- ¹⁸A. Nishimura, S. Matsuda, Y. Kabe, and H. Nakamura, *Jpn. J. Appl. Phys., Part 1* **57**, 07LD23 (2018).
- ¹⁹J. Viard, E. Beche, D. Perarnau, R. Berjoan, and J. Durand, *J. Eur. Ceram. Soc.* **17**, 2025 (1997).
- ²⁰L. G. Parratt, *Phys. Rev.* **95**, 359 (1954).
- ²¹C. Thomsen, J. Strait, Z. Vardeny, H. J. Maris, J. Tauc, and J. J. Hauser, *Phys. Rev. Lett.* **53**, 989 (1984).
- ²²C. Thomsen, H. T. Grah, H. J. Maris, and J. Tauc, *Phys. Rev. B* **34**, 4129 (1986).
- ²³A. Nagakubo, A. Yamamoto, K. Tanigaki, H. Ogi, N. Nakamura, and M. Hirao, *Jpn. J. Appl. Phys., Part 1* **51**, 07GA09 (2012).
- ²⁴A. Devos and R. Côte, *Phys. Rev. B* **70**, 125208 (2004).
- ²⁵H. Ogi, T. Shagawa, N. Nakamura, M. Hirao, H. Odaka, and N. Kihara, *Phys. Rev. B* **78**, 134204 (2008).
- ²⁶A. Nagakubo, H. Ogi, H. Ishida, M. Hirao, T. Yokoyama, and T. Nishihara, *J. Appl. Phys.* **118**, 014307 (2015).
- ²⁷P. Kroll, *J. Non-Cryst. Solids* **293**, 238 (2001).
- ²⁸A. Nagakubo, M. Arita, T. Yokoyama, S. Matsuda, M. Ueda, H. Ogi, and M. Hirao, *Jpn. J. Appl. Phys., Part 1* **54**, 07HD01 (2015).
- ²⁹J. Matsuoka, N. Kitamura, S. Fujinaga, T. Kitaoka, and H. Yamashita, *J. Non-Cryst. Solids* **135**, 86 (1991).
- ³⁰P. N. Sen and M. F. Thorpe, *Phys. Rev. B* **15**, 4030 (1977).
- ³¹F. L. Galeener, *Phys. Rev. B* **19**, 4292 (1979).
- ³²A. E. Geissberger and F. L. Galeener, *Phys. Rev. B* **28**, 3266 (1983).
- ³³M. Knapp, P. Jager, W. Ruile, M. Honal, I. Bleyl, and L. M. Reindl, in *Proceedings of the IEEE Ultrasonics Symposium* (2015), Vol. 1, p. 0112.